Supplementary Material (ESI) for Chemical Communications

Porous Protein Frameworks with Unsaturated Metal Centers in Sterically Encumbered Coordination Sites

Robert J. Radford,[a] Morgan Lawrenz[a,b], Phuong C. Nguyen[a], J. Andrew McCammon[a,b,c,d] and F. Akif Tezcan[a]*

*[a] Department of Chemistry and Biochemistry; [b] Center for Theoretical Biological Physics; [c] Department of Pharmacology; [d] Howard Hughes Medical Institute; University of California, San Diego 9500 Gilman Dr, La Jolla, CA USA, 92037. *E-mail: tezcan@ucsd.edu*

Table of Contents

Section S1. Experimental Details and Procedures

S1.1. Site Directed Mutagenesis and Protein Expression, Purification, Characterization

Site directed mutagenesis was performed on the pETc-b562 plasmid (denoted as wild-type)[1] using the QuikChange kit (Stratagene) and employing primers obtained from Integrated DNA Technologies. The mutant plasmids were transformed into XL-1 Blue *E. coli* cells and purified using the QIAprep Spin Miniprep kit (Qiagen). Point mutations were executed to obtain the following cyt cb_{562} variant: W59C-R62A-H63A-D66A-cyt cb_{562} (MBP). Sequencing of the mutant plasmid was carried out by Retrogen Inc. (San Diego, CA).

The mutant plasmid, isolated from XL-1 blue cells, was transformed into BL21(DE3) *E. coli* cells along with the *ccm* heme maturation gene cassette plasmid, pEC86.[2] Cells were plated on LB agar, containing 100 μg/ml ampicillin and 34 μg/ml chloramphenicol, and grown overnight. LB medium was then inoculated from these colonies and allowed to incubate for 16 hours at 37° C, with rotary shaking at 250 rpm. No induction was necessary.

Mutant-expressing cells were sonicated, brought to pH 5 with the addition of HCl, and centrifuged at 16,000 g, 4° C, for 1 hr. The protein was then purified by ion-exchange chromatography on a CM-Sepharose matrix (Amersham Biosciences) using a NaCl gradient in sodium acetate buffer (pH 5). After exchange into sodium phosphate buffer (pH 8) the protein was further purified using an Uno-Q (BioRad) anion exchange column on a DuoFlow chromatography workstation (BioRad) using a NaCl gradient. Protein purity was determined by SDS-PAGE gel electrophoresis. Verification of mutations was made through MALDI mass spectrometry. MW observed = 12065 amu, MW expected: = 12062 amu.

S1.2. Synthesis of 5-Iodoaceamido-1,10-phenanthroline (IA-Phen)

0.5 g (2.56 mmol) of 5-amino-1-10-phenanthroline (Polysciences) was dissolved in 90 mL of acetonitrile with slight heating. To this stirred solution, the freshly prepared iodoacetic acid anhydride dissolved in 10 mL of acetonitrile was added. The mixture was allowed to react in the dark overnight. The precipitated product was isolated by filtration and washed with cold 5% sodium bicarbonate, followed by water and dried in vacuo. Both the ESI MS and NMR spectra correspond to previously reported literature values.[3] (Yield: 75%)

S1.3. Functionalization of MBP with IA-Phen

A solution of 0.3 mM of MBP, in degassed 0.1 M Tris buffer (pH 7.75), was treated with a 10-fold excess of dithiothreitol (DTT) (Sigma). The protein was allowed to reduce for a period of 30 min. The protein was then dialyzed against 2 x 1 L of degassed 0.1 M Tris buffer (pH 7.75) under an inert atmosphere to remove DTT. A 10-fold excess of IA-Phen was dissolved in 2 mL of degassed DMF and added drop-wise to the protein solution over the course of 1 min. The mixture was allowed to react in the dark at 25° C overnight. The reaction mixture was then dialyzed again against 2 x 1 L of 10 mM sodium phosphate (pH 8) and 1 mM EDTA. The crude labeled protein was subsequently purified on an Uno-Q anion-exchange column (BioRad) using an NaCl gradient. The purity of the functionalized protein was determined by MALDI mass

spectrometry and SDS-PAGE electrophoresis (Labeling yield: 85-95%). MW observed = 12300 amu, MW expected = 12298 amu).

S1.4. Crystallography

General

All crystals were obtained by sitting drop vapor diffusion using a Hampton 24-well sitting drop plate. All reagents were of the highest possible purity commercially available. Solutions and reagents were filtered using a 0.2 micron cellulose membrane filter prior to use. Unless otherwise noted, the crystals to be used for diffraction experiments were exchanged into a solution containing 20% glycerol as a cryoprotectant. X-ray diffraction data for all crystals were collected at 100 K at Stanford Synchrotron Radiation Laboratory (BL 9-2 or BL 7-1) using 0.98 Å radiation. The data were processed using MOSFLM and SCALA.[4]

The initial molecular replacement solution for all crystals was determined by PHASER,[5] using the cyt cb_{562} structure (PDB ID 2BC5)[6] as the search model. The search model for each crystal form did not contain the heme or the Phen prosthetic groups; the observation of strong positive F_o-F_c density at expected positions for these groups confirmed the correct placement of protein monomers. The topology and parameter files for the phenanthroline group were obtained using the Dundee ProDrg Server (http://davapc1.bioch.dundee. ac.uk/prodrg/index.html). Rigid-body, positional and thermal refinement with REFMAC,[4, 7] along with manual rebuilding, and water placement with COOT[8] produced the final models. All figures were produced with PYMOL.[9]

MBPPhen2

MBPPhen2 was crystallized at 25° C with a premade Hampton screen precipitation solution (HR2-144, #24) consisting of 2.8 M sodium acetate trihydrate (pH 7.0). The drop consisted of 2 μL of protein (2.6 mM in 20 mM Tris (pH 7) and 1 mM EDTA) and 1 μL of the precipitation solution. Crystals appeared within 2 months reaching a maximum size of ~ 300 μm × 300 μm × 500 μm. The crystals used in diffraction experiments were frozen directly in liquid N_2 without addition of a cryoprotectant. The structure was determined to 2.01-Å resolution (PDB: 3NMI) (Table S1).

Ni:MBP-Phen2

Ni:MBPPhen2$_2$ was crystallized at 25° C with a precipitation solution consisting of 0.1 M Tris (pH 8.5), 0.2 M ammonium sulfate, 30% PEG 400 and 6.2 mM nickel sulfate. The drop consisted of 2 μL of protein (3.1 mM in 20 mM Tris (pH 7)) and 1 μL of the precipitation solution. Crystals appeared within 1 months reaching a maximum size of ~ 100 μm × 200 μm × 200 μm. The crystals used in diffraction experiments were exchanged into cryoprotecting solution and frozen in liquid N_2. The structure was determined at 3.10 Å resolution (PDB: 3NMJ) (Table S1).

Zn:MBP-Phen2

Zn:MBPPhen2$_2$ was crystallized at 25° C with precipitation solution consisting of 0.1 M Tris (pH 8.5), 0.2 M ammonium sulfate and 30% PEG 400 and 12.4 mM zinc chloride. The drop consisted of 2 μL of protein (3.1 mM in 20 mM Tris (pH 7)) and 1 μL of the precipitation solution. Crystals appeared within 1 months reaching a maximum size of ~ 100 μm × 200 μm ×

200 μm. The crystals used in diffraction experiments were exchanged into cryoprotecting solution and frozen in liquid N_2. The structure was determined to 2.85-Å resolution (PDB: 3NMK) (Table S1).

Crosslinking Ni:MBPPhen2$_2$ crystals with Glutaraldehyde

Ni:MBPPhen2 crystals (~6) were added to a 12 μL of the precipitation solution (see above) and 4 μL of a 25% gultaraldehyde grade II solution (Sigma). The crystals were allowed to crosslink for 30 min, after which they were washed 3 times by placing them in successive 20 μL solutions of fresh precipitant solution. Although the unit cell was not determined, the integrity of the crystals was continuously checked by their ability to polarize light.

S1.5. Sedimentation Velocity Experiments

Sedimentation velocity (SV) experiments were performed in order to determine the solution-state oligomerization behavior of MBPPhen2. All SV samples were prepared in 20 mM Tris buffer (pH 7). Measurements were made on a Beckman XL-I Analytical Ultracentrifuge (Beckman-Coulter Instruments) using an An-60 Ti rotor at 41,000 rpm for a total of 250 scans/sample at a wavelength of 664 nm (600 μM protein).

All data were processed using SEDFIT.[10] Buffer viscosity, buffer density, and protein partial specific volume values were calculated at 25° C with SEDNTERP (http://www.jphilo.mailway.com). Partial specific volume (Vbar) for HQuin1 mutant was calculated to be 0.7360 mg/ml, assuming a partial specific volume of heme of 0.82 mg/ml and 0.71 mg/ml for the phenanthroline.[11] All data were processed using fixed values for buffer density (ρ) (0.99764 g/ml) and buffer viscosity (0.0089485 poise).

S1.6. Computational Calculations and Simulations

Free Energy Calculation for Phen Burial

To determine the solvation free energy difference between the "in," stacked Phen conformation observed in MBP-Phen2 complex and the more solvent exposed "out" conformation in the MBP-Phen2 conformation, alchemical free energy calculations were performed using NAMD2.7β1. These calculations utilize unphysical intermediate states, in which the non-bonded potential energy terms for the Phen residue are linearly scaled to zero with the parameter λ, as represented in Figure S3.3. This decoupling[12] of the residue from its environment in both the "in" and "out" conformations allows computation of a relative solvation free energy difference $G_{out\#\ in}$, as depicted in the thermodynamic cycle of Figure S3.3.

The decoupling steps for computation of G_{in} and G_{out} in Figure S3.3 were performed over 14 windows of λ (λ=0.0, 0.05, 0.1, 0.15, 0.2, 0.25, 0.3, 0.4, 0.5, 0.6, 0.7, 0.8, 0.9,1.0), with electrostatic potential terms scaled to zero by window 7, and van der Waals potential terms annihilated by window 14. A softcore potential[13] was used for annihilation of the van der Waals potentials to improve convergence and accuracy of the calculation. For simulations of the

complex at each window of λ, a 1 ns equilibration period precedes a 1 ns sampling period, during which values of $\left\langle \frac{dV}{d\lambda} \right\rangle_\lambda$ were computed every 5 timesteps for thermodynamic integration:[14]

$$\Delta G = \int_0^1 \left\langle \frac{dV}{d\lambda} \right\rangle_\lambda d\lambda$$

where V is the total potential energy of the system, and the average derivative is computed over the simulation time at each λ window. The integral is evaluated using cubic spline integration from λ=0, when the atoms of Phen are fully coupled, to λ=1, when the atoms do not interact with the rest of the system.

To restrict conformational sampling to the relevant conformational states of the Phen residue in the MBP-Phen1 and MBP-Phen2 complexes, a harmonic restraint potential $U_{COM} = k(r_{COM} - r_0)^2$ was applied to the Phen center of mass (COM), with a reference COM position r_0 and magnitude of the harmonic constant $k = \frac{3RT}{\left\langle \delta r_{COM}^2 \right\rangle}$ determined from the average COM position and average fluctuation $\left\langle \delta r_{COM}^2 \right\rangle$ over 2 ns NPT (at T=300 K) simulations of both complexes. A relative free energy difference between these two conformations, $\Delta\Delta G_{out \to in}$ was found by subtracting ΔG_{in} from ΔG_{out}, as in Scheme SX. A bootstrapping re-sampling method was employed to obtain variances for the $\left\langle \frac{dV}{d\lambda} \right\rangle_\lambda$ values, which were then propagated in the integration to give the uncertainty reported for $\Delta\Delta G_{out \to in}$.

S2. Experimental Tables

X-ray data collection and refinement statistics			
	MBP-Phen2	**Ni:MBP-Phen2**	**Zn:MBP-Phen2**
Data collection location	SSRL BL 9-2	SSRL BL 7-1	SSRL BL 7-1
Unit cell dimensions (Å)	88.29 × 91.79 × 130.64 α = 90° ß= 108°, γ =90°	99.29 × 99.29 × 109.32 α =ß = 90°, γ = 120.0°	99.46 × 99.46 × 109.54 α =ß = 90°, γ = 120.0°
Symmetry group	*C*2	$P6_5$	$P6_5$
Resolution (Å)	2.01	3.10	2.80
X-ray wavelength (Å)	0.979	0.979	0.979
Number of unique reflections	65484	11200	15237
Redundancy	4.4	9.9	7.7
Completeness (%)*	99.7	100.0	99.9
⟨I / σI⟩*	1.7	1.4	1.9
R_{symm}‡* (%)	23.7	43.3	30.1
R_{work}§/R_{free}II (%)	19.8 / 23.5	19.3 / 23.8	18.8 / 23.3
Contents of asu			
Protein monomers	6	4	4
Ligands/ions	6 / 5	4 / 2	4 / 2
Water	285	4	32
R.m.s deviations¶			
Bond lengths (Å)	0.009	0.006	0.007
Bond angles (°)	0.985	0.742	0.814

Table S2.1. X-ray data collection and refinement statistics for: MBP-Phen2, Ni:MBP-Phen2 and Zn:MBP-Phen2.

*Numbers in parentheses correspond to the highest resolution shell: (2.120 - 2.010 Å) for EDTA:MBP-Phen2, (3.270 – 3.100 Å) for Ni:MBP-Phen2, and (2.950 – 2.800 Å) for Zn:MBP-Phen2, respectively

‡ $R_{sym}= \Sigma\Sigma_j| I_j-\langle I\rangle| /\Sigma\Sigma_j| I_j|$.

§ $R= \Sigma|\,|F_{obs}|-|F_{calc}|\,|/\Sigma|F_{obs}|$

IIFree R calculated against 7 of the reflections removed at random.

¶Root mean square deviations from bond and angle restraints.

S3. Experimental Figures

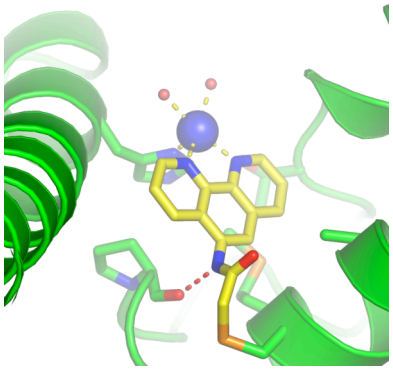

Figure S3.1. Inner sphere coordination environment in the trimeric Ni:MBPPhen1$_3$ complex, highlighting the coordinatively unsaturated Ni^{2+} center.

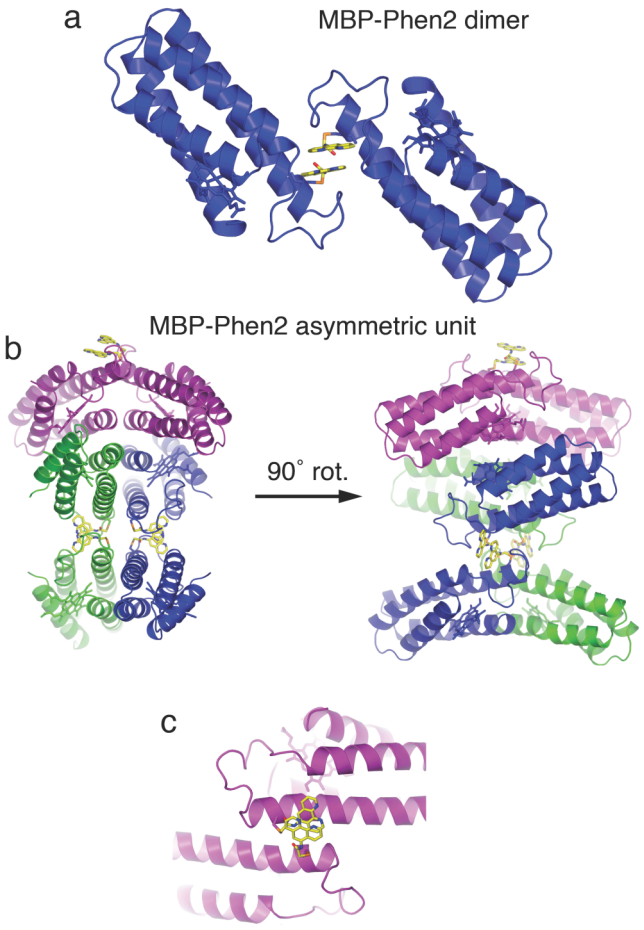

Figure S3.2. Various views of the metal free MBPPhen2 crystal structure. (a) The head-to-head aligned pair of MBPPhen molecules the feature π-stacked Phen groups, as shown in detail in Figure 2 in the Main Text. (b) Contents of the asymmetric unit in MBPPhen2 crystals. Each MBPPhen2 pair whose Phen groups are found in association are colored alike. (c) Closeup view of the two Phen groups found in the "out" conformation.

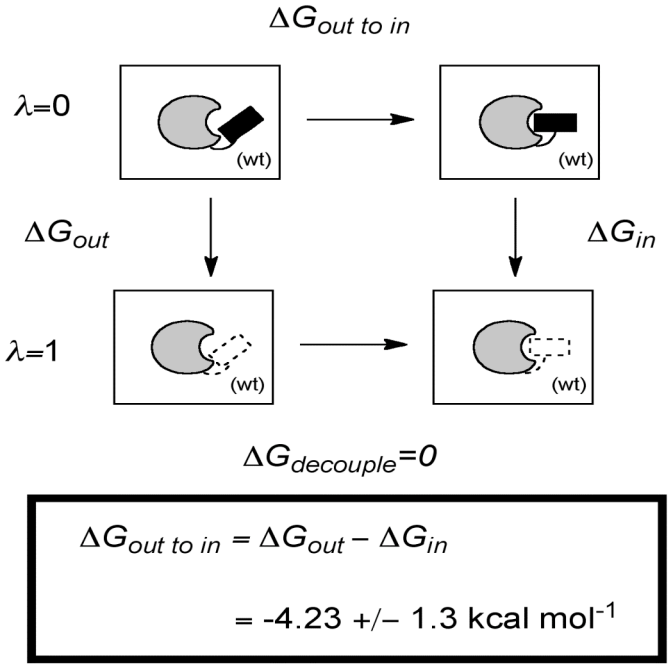

Figure 3.3. Cartoon representing the thermodynamic cycle for computing the free energy difference between the two conformations of the Phen residue in MBPPhen2. At λ=1 the nonbonding potential terms of the Phen have been turned off, decoupling the residue from its environment.

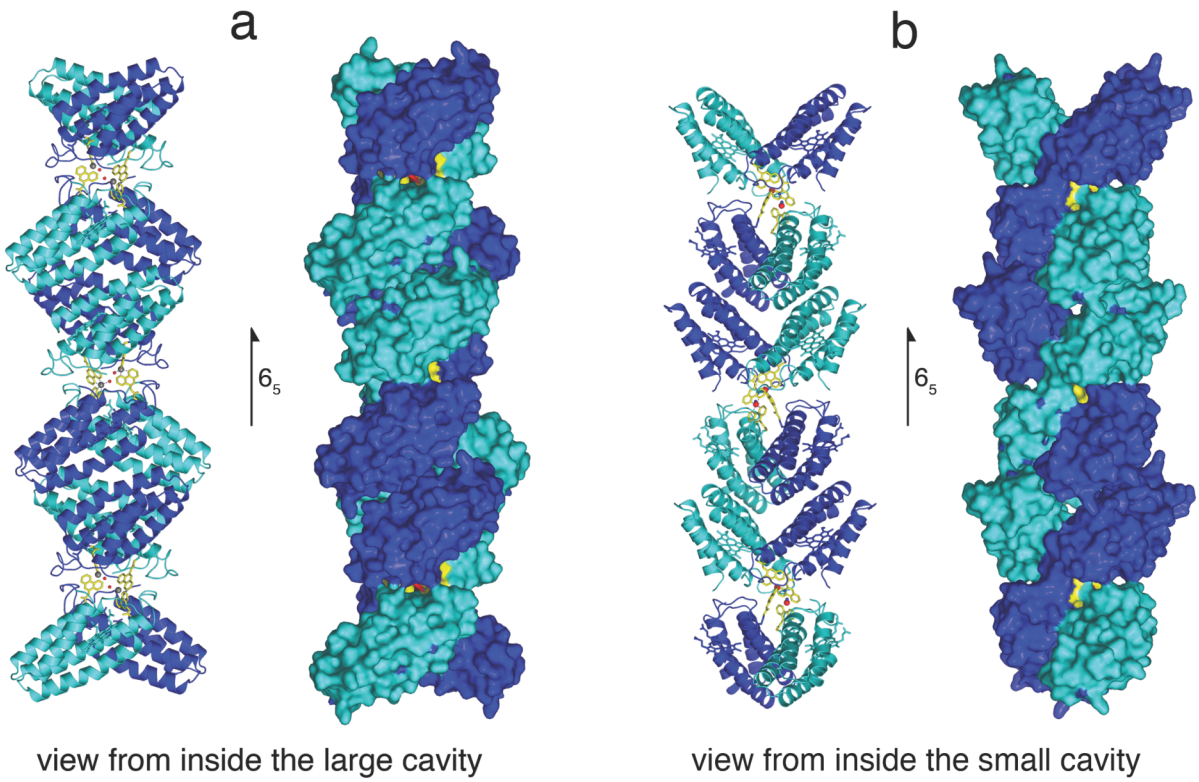

Figure S3.4. Columns of Zn:MBPPhen2_2 molecules that form the lining of the hexagonal pores in the crystal lattice, shown in ribbon and surface representations. The orientation of each column as seen from inside (a) the large pores (see Figure 4 in the Main Text) and (b) the small pores.

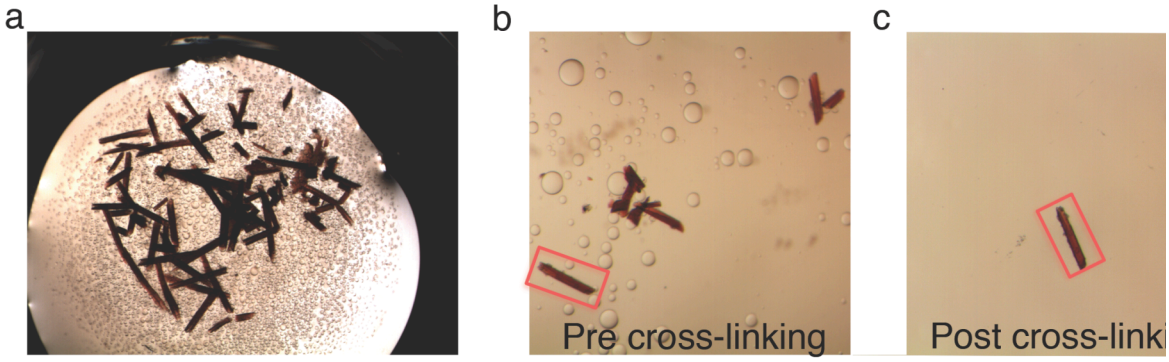

Figure S3.5. Crosslinking of Ni:MBPPhen2$_2$ crystals with glutaraldehyde. (a) Ni:MBPPhen2$_2$ crystals in the crystallization well. (b) Ni:MBPPhen2$_2$ crystals in precipitation solutions prior to crosslinking. (c) Sample Ni:MBPPhen2$_2$ crystal in water after cross-linking. The crosslinked crystal shown in (c) is highlighted with a red box in (b) for comparison.

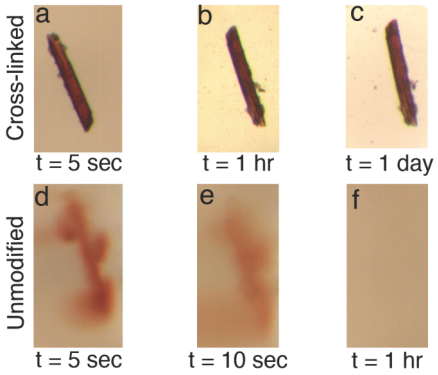

Figure S3.6. Comparing stability of crosslinked and unmodified Ni:MBPPhen2$_2$ crystals in H_2O (no precipitant). Crosslinked Ni:MBPPhen2$_2$ crystals display no noticeable deterioration after (a) 5 sec (b) 1 hr, or (c) 1 day. Conversely, unmodified Ni:MBPPhen2$_2$ crystals begin dissolving almost immediately under the same conditions ((d) 5 sec, (e) 10 sec) and are completely dissolved after a period of (f) 1 hr.

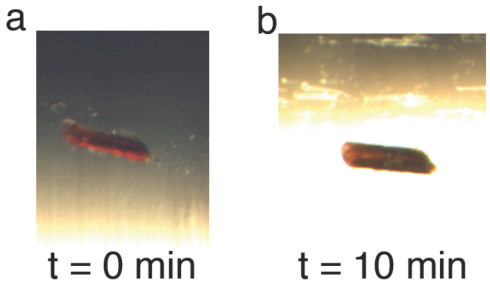

Figure S3.7. Monitoring the effect of high temperatures on crosslinked Ni:MBPPhen2$_2$ crystals. Ni:MBP-Phen2 crystals were placed in a thin walled Eppendorf tube and held at 98° C for 10 min. (a) prior to heating, (b) after heating.

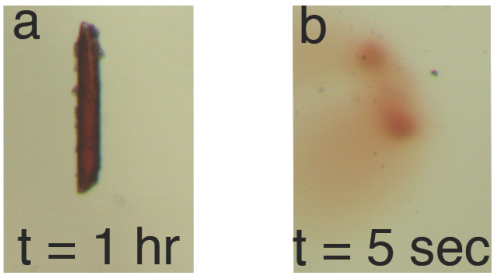

Figure S3.8. Effect of organic solvent on cross-linked and unmodified Ni:MBPPhen2$_2$ crystals. (a) No visible changes are seen after exposure of crosslinked Ni:MBPPhen2$_2$ crystals to 50% (v/v) H_2O/Acetonitrile. (b) In contrast, unmodified Ni:MBPPhen2$_2$ crystals immediately dissolve upon exposure to the same solvent.

S4. References

1. J. Faraone-Mennella, H. B. Gray and J. R. Winkler, *Proc. Natl. Acad. Sci. USA*, 2005, 102, 6315-6319.
2. M. Braun and L. Thony-Meyer, *Proc. Natl. Acad. Sci. USA*, 2004, 101, 12830-12835.
3. F. N. Castellano, J. D. Dattelbaum and J. R. Lakowicz, *Anal. Biochem.*, 1998, 255, 165-170.
4. Collaborative Computational Project, Number 4. 1994. "The CCP4 Suite: Programs for Protein Crystallography". Acta Cryst. D50, 760-763
5. A. J. McCoy, R. W. Grosse-Kunstleve, P. D. Adams, M. D. Winn, L. C. Storoni and R. J. Read, *J. Appl. Crystallogr.*, 2007, 40, 658-674.
6. J. T. Faraone-Mennella, F. A.; Gray, H. B.; Winkler, J. R., *Biochemistry*, 2006, 45, 10504-10511.
7. G. Murshudov, A. Vagin and E. Dodson, *Acta Cryst.*, 1996, D53, 240-255.
8. P. Emsley and K. Cowtan, *Acta Cryst.*, 2004, D60, 2126-2132.
9. W. L. DeLano, *The PYMOL Molecular Graphics System (http://www.pymol.org)*, 2003.
10. P. Schuck, *Biophys. Chem.*, 2004, 108, 187-200.
11. Calculated using Advanced Chemistry Development (ACD/Labs) Software V8.14 for Solaris (© 1994-2009 ACD/Labs).
12. M. K. Gilson, J. A. Given, B. L. Bush and J. A. McCammon, *Biophys. J.*, 1997, 72, 1047-1069.
13. T. C. Beutler, A. E. Mark, R. C. van Schaik, P. R. Gerber and W. F. van Gunsteren, *Chem. Phys. Lett.*, 1994, 222, 529-539.
14. J. G. Kirkwood, *J. Chem. Phys.*, 1935, 3, 300-313.